DNA AND CELL BIOLOGY
Volume 30, Number 11, 2011

Pp. 851–864
DOI: 10.1089/dna.2011.1315

The Bladder Tumor Suppressor Protein TERE1 (UBIAD1) Modulates Cell Cholesterol: Implications for Tumor Progression

William J. Fredericks,[1] Terry McGarvey,[2] Huiyi Wang,[1] Priti Lal,[3] Raghunath Puthiyaveettil,[3] John Tomaszewski,[3] Jorge Sepulveda,[3,5] Ed Labelle,[6] Jayne S. Weiss,[7] Michael L. Nickerson,[8] Howard S. Kruth,[9] Wolfgang Brandt,[10] Ludger A. Wessjohann,[10] and S. Bruce Malkowicz[1,4]

Convergent evidence implicates the TERE1 protein in human bladder tumor progression and lipid metabolism. Previously, reduced TERE1 expression was found in invasive urologic cancers and inhibited cell growth upon re-expression. A role in lipid metabolism was suggested by TERE1 binding to APOE, a cholesterol carrier, and to TBL2, a candidate protein in triglyceride disorders. Natural *TERE1* mutations associate with Schnyder's corneal dystrophy, characterized by lipid accumulation. TERE1 catalyzes menaquinone synthesis, known to affect cholesterol homeostasis. To explore this relationship, we altered TERE1 and TBL2 dosage via ectopic expression and interfering RNA and measured cholesterol by Amplex red. Protein interactions of wild-type and mutant TERE1 with GST-APOE were evaluated by binding assays and molecular modeling. We conducted a bladder tumor microarray TERE1 expression analysis and assayed tumorigenicity of J82 cells ectopically expressing TERE1. TERE1 expression was reduced in a third of invasive specimens. Ectopic TERE1 expression in J82 bladder cancer cells dramatically inhibited nude mouse tumorigenesis. TERE1 and TBL2 proteins inversely modulated cellular cholesterol in HEK293 and bladder cancer cells from 20% to 50%. TERE1 point mutations affected APOE interactions, and resulted in cholesterol levels that differed from wild type. Elevated tumor cell cholesterol is known to affect apoptosis and growth signaling; thus, loss of TERE1 in invasive bladder cancer may represent a defect in menaquinone-mediated cholesterol homeostasis that contributes to progression.

Introduction

Bladder carcinoma is the fifth most common non-cutaneous solid malignancy in the United States and was associated with 70,980 new cases and over 14,330 deaths in 2010 (ACS, 2010). The majority (90%) are classified as transitional cell carcinoma (TCC). Among patients with invasive or advanced disease, therapy consists of radical surgery and/or chemotherapy, which can achieve an overall 5-year survival rate of barely 50%. Those patients with advanced disease have a less than 10% sustained complete response from chemotherapy. There is clearly significant room for a greater understanding of new factors involved in disease progression that may lead to improvement in the treatment of muscle invasive disease (Sanchez-Carbayo and Cordon-Cardo, 2007).

We have investigated a role for the TERE1 protein (also referred to as UBIAD1) in tumor cell metabolism associated with an invasive phenotype based on key observations relating to protein interaction, disease associations, and expression levels. Preliminary studies found that TERE1 message and protein expression was reduced in human bladder cancer specimens and a set of metastatic prostate cancer specimens (McGarvey *et al.*, 2001, 2003). TERE1 overexpression inhibited growth of transitional cell carcinoma cell lines J82 and HT1376, and prostate cancer cell lines PC3 and LnCaP (McGarvey *et al.*, 2001, 2003). A possible relationship between TERE1 and cellular lipids was recog-

[1]Division of Urology, Department of Surgery, University of Pennsylvania, Philadelphia, Pennsylvania.
[2]Department of Anatomy, Kirksville Osteopathic Medical School, Kirksville, Missouri.
[3]Department of Pathology and Laboratory Medicine, University of Pennsylvania School of Medicine, Philadelphia, Pennsylvania.
[4]Department of Surgery of Urology, and Pathology, Veterans Affairs Medical Center Philadelphia, Philadelphia, Pennsylvania.
[5]Pathology Service, Veteran's Affairs Medical Center Philadelphia, Philadelphia, Pennsylvania.
[6]Gloucester County College, Sewell, New Jersey.
[7]Department of Ophthalmology and Eye Center, Louisiana State University, New Orleans, Louisiana.
[8]Cancer and Inflammation Program, National Cancer Institute, Frederick, Maryland.
[9]Section of Experimental Atherosclerosis, National Heart, Lung, and Blood Institute, National Institutes of Health, Bethesda, Maryland.
[10]Leibniz Institute of Plant Biochemistry, Halle, Germany.

nized via the interaction of TERE1 with the APOE cholesterol carrier protein (McGarvey *et al.*, 2005) and further supported by *TERE1* mutations in Schnyder's corneal dystrophy (SCD), a rare disease of corneal cell cholesterol and lipid accumulation (Weiss *et al.*, 2007; Nickerson *et al.*, 2010). TERE1 expression has been reported to be mitochondrial and or in endoplasmic reticulum in different cell types (Nakagawa *et al.*, 2010; Nickerson *et al.*, 2010). Recently, TERE1-mediated prenyltransferase activity in vitamin K-2 synthesis was demonstrated, and vitamin K-3 was shown to be an intermediate during conversion of K-1 to K-2 (Nakagawa *et al.*, 2010). Vitamin K-1 has a well-known role as a cofactor for gamma glutamyl carboxylase, GGCX, which carboxylates glutamine residues in vitamin K-dependent factors important in clotting (Merli and Fink, 2008; Shearer and Newman, 2008). Vitamin K also plays a role in bone health (Bugel, 2008), and acts as a cofactor for the GAS6 ligand for several receptor tyrosine kinases (Lamson and Plaza, 2003; Bellido-martin and Defrutos, 2008). Most relevant to TERE1 and tumor cell biology is that vitamin K-2, menaquinone, and vitamin K-3, also known as menadione, are redox-cycling and alkylating quinones known to inhibit growth of different types of tumor cell lines (Nishikawa *et al.*, 1999; Lamson and Plaza, 2003; Jamison *et al.*, 2004; Bandyopadhyay, 2008; Shearer and Newman, 2008; Amalia *et al.*, 2010; Gilloteaux *et al.*, 2010). Vitamin K-2 is also known to activate SXR signaling and cause diverse effects, including modulation of lipid homeostasis via cholesterol efflux (Shearer and Newman, 2008; Zhou *et al.*, 2009). This represents a potentially significant breakthrough in understanding TERE1 modulation of tumor cell metabolism since it may link the oxidative stress of quinone redox to cholesterol homeostasis.

In addition, TERE1 also binds to the TBL2 protein, which has been implicated in disease associated with triglyceride metabolism (Kathiresan *et al.*, 2008; Wang *et al.*, 2008a). *TBL2* was originally described as a gene within a chromosomal deletion in Williams Syndrome (Perez Jurado *et al.*, 1999). The TBL2 protein has a single transmembrane domain, five WD40 domains, and a putative nuclear localization signal. A role for TBL2 in TGFβ signaling was suggested via interaction with the SMURF1 ubiquitin ligase (Barrios-Rodiles *et al.*, 2005). TBL2 was also found to undergo phosphorylation at T433 by ATM/ATR in response to oxidative DNA damage (Matsuoka *et al.*, 2007). Recently, TBL2 was found to bind to PDK1, implying a possible role in AKT signaling (Behrends *et al.*, 2010). Together, these studies point to a role for TERE1 and TBL2 as potential modulators of cell stress and growth signaling, and lipid metabolism.

A role for elevated cholesterol has been implicated in the etiology and disease progression in prostate and breast cancer, with emphasis on its role as a precursor to steroid metabolism and intracrine growth mechanisms (Di Vizio *et al.*, 2008; Twiddy *et al.*, 2010). However, there is also a separate recognition that elevated intracellular cholesterol in non-hormone-dependent tumor cells can contribute to progression based on numerous reports of interference with multiple pathways of growth signaling and apoptosis (Zhuang *et al.*, 2005; Li *et al.*, 2006; Swinnen *et al.*, 2006; Adam *et al.*, 2007; Freeman *et al.*, 2007; Martinez-Abundis *et al.*, 2007; Oh *et al.*, 2007; Christenson *et al.*, 2008; Patra, 2008). The link between intracellular cholesterol and tumor progression has been found in hepatocellular carcinoma, colon, breast, head and neck, and melanoma cancers, either with tumor specimens and/or studies in cancer cell lines (Schabath *et al.*, 2006; Baruthio *et al.*, 2008; Montero *et al.*, 2008). As an essential component for cell membranes required for tumor cell proliferation, and as a central modulator of membrane signaling complexes for growth, oxidative stress management, and apoptosis, altered cholesterol has potential for simultaneously affecting multiple facets of tumor progression.

The principle objectives of this study were to confirm the TERE1-negative expression phenotype in a third of advanced lesions from a tumor microarray (TMA) set of human bladder tumor specimens and to demonstrate the inhibitory effects of ectopic TERE1 expression on tumorigenic growth of the J82 TCC cell line in nude mice. Further, we show that altering the dosage of the TERE1 and TBL2 proteins modulates intracellular cholesterol and that mutations in TERE1 associated with SCD can interfere with binding to APOE. We discuss implications of TERE1 in the context of future understanding of mechanisms of tumor progression in bladder and other cancers.

Materials and Methods

Cell lines and antibodies

All cell lines were obtained from the American Type Culture Collection and grown according to supplier's instructions. Polyclonal antibodies against specific peptide antigens of the human TERE1 (amino acids 31–45, 229–242, 301–314) and TBL2 (amino acids 111–129, 353–366, 413–426) proteins were prepared in rabbits or chickens at Invitrogen and were antigen affinity purified according to standard methods. Goat anti-TERE1 antibodies were obtained from Santa Cruz. Rabbit anti-TBL2 (216–309) and hrp-mouse-anti-FLAG-M2 were obtained from Sigma.

Expression vectors

The pcDNA3.1HisC-*TERE1* plasmid and the pTRE-REV-*TERE1* retrovirus plasmids were previously described (McGarvey *et al.*, 2001, 2003, 2005). The mammalian CMV expression plasmids pM12-NFLAG-*TERE1* and pM12-NFLAG-*TBL2* were obtained from GeneCopoeia. The pAd/CMV/V5DEST-*TERE1* adenovirus plasmid was derived using Gateway LR recombination with a pDONR221-*TERE1* entry plasmid following recommendations from Invitrogen. pAd/CMV/GFP plasmid was from Clontech. Site-directed point and stop mutations in *TERE1* and *TBL2* were constructed using the Stratagene quickchange XL mutagenesis strategy with pM12-NFLAG-*TERE1* and pM12-NFLAG-*TBL2* plasmids as templates and appropriate mutagenic primers as specified by the manufacturer. The mammalian micro-RNA (miRNA) expression plasmids for NM_013319.1_*TERE1* #7–12 and NM_012453_*TBL2* #1–6 were constructed in pcDNA6.2 EmGFP MiR entry vectors (Invitogen) by standard PCR cloning of annealed oligonucleotide 64-mers followed by a two-step (BP, then LR) Gateway recombination to transfer the miRNA cassettes to pAdV5DEST adenoviral and pLenti 6.2 lentiviral plasmids following detailed specifications from Invitrogen. The oligonucleotide 64-mer sequences were MiR *TBL2*-1, 5′ CCTGTGCACAGGTAGAGGTATTTGTCAGTCAGTGGCC AAAACAAATACCTGGCTACCTGTGCAC 3′; MiR *TBL2*-2, 5′ CCTGAGACGATGAAGTCTGCAGTGTCAGTCAGTGG

CCAAAACACTGCAGAGCCTTCATCGTCTC 3′; MiR *TBL2*-3, 5′ CCTGTCATCTTGAAGACGGAGGGGTCAGTC AGTGGCCAAAACCCCTCCGTGTCTTCAAGATGAC 3′; MiR *TBL2*-4, 5′ CCTGTTCCAAAGCAGTTCCCAAAGTCA GTCAGTGGCCAAAACTTTGGGAAGTCTGCTTTGGAAC 3′; MiR *TBL2*-5, 5′ CCTGAGTCGTTGGAGAGCAAACGGTCA GTCAGTGGCCAAAACCGTTTGCTTTCTCCAACGACTC 3′; MiR *TBL2*-6, 5′ CCTGTAGAGATGAATTACTGCCAGTCAG TCAGTGGCCAAAACTGGCAGTAGTATTCATCTCTAC 3′; MiR *TERE1*-7, 5′ CCTGAAAGTGAGCCACACAGTGAGTCA GTCAGTGGCCAAAACTCACTGTGCGTGGCTCACTTTC 3′; MiR *TERE1*-8, 5′ CCTGAGCTTTGACAGTCTCCCGAGTCAG TCAGTGGCCAAAACTCGGGAGAGACTGTCAAAGCTC 3′; MiR *TERE1*-9, 5′ CCTGTAAGTGTTGACAATTACCGGTCAG TCAGTGGCCAAAACCGGTAATTTGGTCAACACTTAC 3′; MiR *TERE1*-10, 5′ CCTGCAAAGTAGATAAGCCAAGTGTCA GTCAGTGGCCAAAACACTTGGCTCTTATCTACTTTGC 3′; MiR *TERE1*-11, 5′ CCTGTTGGAATGGAGTGGCCTCGGTC AGTCAGTGGCCAAAACCGAGGCCATTCTCCATTCCA AC 3′; and MiR *TERE1*-12, 5′ CCTGTTCTAAGAAAGAGA CATGTGTCAGTCAGTGGCCAAAACACATGTCTCCCTTT CTTAGAAC 3′. miRNA plasmids were screened for loss of β-galactosidase activity from cotransfected LACZ-*TERE1* and LACZ-*TBL2* target cDNA fusions and also by loss of expression of cotransfected *TERE1* and *TBL2* (data not shown). The *TERE1* and *TBL2* miRNAs were tested in both pcDNA6.2 and pLenti6.3/V5DEST CMV vectors in comparison to empty vector and scrambled sequence MiR-NC-negative control plasmids. The bacterial expression plasmid pB04-GST-*APOE* was obtained from GeneCopoeia. Infectious adenovirus was produced and amplified in HEK293A cells following guidelines from Invitrogen and titered via an anti-hexon staining procedure from Clontech to $>4\times108$ IU/mL. Infections were in the presence of 6 μg/mL polybrene and monitored via Ad*GFP* expression. All plasmids were sequenced to verify coding sequences, point and deletion mutations, reading frames, and were amplified and purified by standard techniques. Plasmids were quantified by UV and Picogreen assay (Invitrogen) and evaluated on ETBr-stained agarose gels.

Transient transfection/expression analysis

Cell lines were transfected with the Nucleofector II system according to the manufacturer's protocol using program Q001 and solution S for HEK293 cells, and program×005 and solution R for J82 cells (Amaxa/Lonza Cologne). The transfection efficiency for HEK293 cells was >95% and for J82 bladder cancer cells was >50%. Viability via trypan blue staining was over 90% in both cases. Expression plasmids were controlled with parallel transfections of CMV empty vector. Cells were grown in 10 cm dishes and harvested after 1–3 days by washing in ice cold PBS, and scraping in presence of protease inhibitors to freeze cell pellets.

Preparation of cell extracts

Whole cell extracts were prepared by lysis of cell pellets in four pellet volumes of a 2% detergent mixture of CHAPS, NP-40 (Calbiochem), BRIJ 96/99 (1:1), and Triton-X-100 (Sigma), containing 150 mM NaCl, 10 mM Tris-HCl (pH 7.4), and protease inhibitors: 1.0 mM EDTA, 2 μg/mL leupeptin and pepstatin, 10 μg/mL aprotinin, and 1.0 mM phenylmethylsulfonlyfluoride, and one complete mini protease inhibitor cocktail tablet (Roche) per 10 mL lysis buffer. After brief sonication, lysates were clarified at 16,000 *g* for 30 min at 4°C and supernatants were evaluated for protein concentration by BCA assay using BSA as a standard. Equal amounts of cell lysate (50 μg of protein) were fractionated by SDS-PAGE in 4%–20% Bis-Tris gels (Invitrogen) run with 2-(N-morpholino) ethane sulfonic acid (MES) buffer under reducing conditions and were transferred to nitrocellulose membranes. The non-specific protein binding sites on blots were blocked by incubation in 5% nonfat dry milk in TBS (150 mM NaCl, 10 mM Tris-HCl [pH 7.4]), and then blots were probed for 2 h at room temperature with affinity purified primary antibodies at ~0.2 μg/mL in TBS pH 7.4 with 3% nonfat dry milk and 0.05% Tween-20. Horseradish peroxidase-conjugated secondary antibodies were used to detect immune complexes on immunoblots. Blots were treated with Supersignal West Pico chemiluminescence reagents (Pierce) and were observed on X ray film (Kodak; Biomax-MR, or Thermo CL-X Posure film).

GST-association assays

We purified GST-vector, and GST-APOE fusion proteins to use as bait in binding assays with wild-type or SCD mutant Flag-tagged TERE1 protein lysates. For the deletion analysis, stop codons were engineered to at Y174 and E242 of TERE1 and Y174 and E311 of TBL2. We adjusted baits to ensure equivalent loading and verified similar expression levels of the FLAG-TERE1 test proteins in HEK293 cell lysates. Expression of the purified GST baits was estimated from Coomassie blue-stained gels and/or immunoblot analysis to normalize the amounts used during associations by filling with empty beads as previously described (Ryan *et al.*, 1999). Test lysates were diluted in association buffer AB (40 mM Tris pH 7.5, 150 mM NaCl, 10% glycerol, 0.2% NP-40, 0.5% BSA plus PIN) and precleared via 1 h incubation with empty GST beads. Equal amounts of GST fusion proteins were incubated with precleared test protein lysates in AB for 2 h at room temperature with continuous gentle mixing, followed by standard centrifugation at 500 *g* for 5 min at 4°C. Beads were given sequential 10 min washes followed by standard centrifugation as follows: once with BB100, three times with BB500, and two times with BB100, and then eluted in SDS-PAGE sample buffer. After SDS-PAGE, bound complexes were analyzed via probing immunoblots with hrp-anti-Flag M2 antibody.

Immunohistochemistry

Five-micron sections from formalin-fixed paraffin-embedded tissue specimens were deparaffinized in xylene and rehydrated in graded alcohol with quenching of endogenous peroxidase activity by treatment with 2% H_2O_2 in methanol. The slides were blocked in 10% normal rabbit serum and incubated with affinity-purified anti-TERE1 (2 μg/mL) for 14 h at 4°C. After washes, the slides were incubated with biotin-conjugated rabbit IgG for 30 min followed by streptavidin-conjugated peroxidase and 3′3-diaminobenzidine, and counterstained with hematoxylin.

Molecular modeling

Based on the model of UBIAD1 (Nickerson *et al.*, 2010) a protein–protein docking was performed with ClusPro

(http://nrc.bu.edu/cluster/) (Comeau *et al.*, 2004a, 2004b) to investigate possible interactions between UBIAD1 and Apoliprotein E3. For this purpose the X-ray structure of the Apolipoprotein E3 22Kd Fragment Lys146Gln Mutant (PDB entry 1H7I) (Rupp *et al.*, to be published) was used. The resulting complex was refined by a molecular dynamics simulation of the entire complex for 500 ps using the md-refinement option embedded in the YASARA molecular modeling software suite (www.yasara.org/).

Cholesterol assay

Cholesterol content of cell lysates was detected using an Amplex red Cholesterol Assay kit relative to a dilution series of cholesterol standards as specified (Invitrogen). The assay was also used to detect H_2O_2 by leaving out cholesterol esterase (CE) and cholesterol oxidase (CO).

Statistical analysis

The values of experimental samples of TERE1 or TBL2 expression vectors were compared to control vector and are presented as the mean ± SD. The means of the two groups were compared by a Student's *t*-test of independent data sets (two samples, two tailed) using the BioToolKit 320 software (BioDataFit 1.02; Chang Bioscience, Inc.). A value of $p < 0.01$ was regarded as significant.

Results

Features of TERE1 protein

The role of TERE1 in synthesis of vitamin K-2 (aka, menaquinone, or MK-4) from vitamin K-1, K-2, and K-3, is consistent with its sequence homology to the bacterial prenyltransferase enzyme MenA (Brauer *et al.*, 2008; Nakagawa *et al.*, 2010; Suvarna *et al.*, 1998). A diagram of the 338 amino acid mitochondrial TERE1 protein showing 10 trans-membrane α-helical domains and illustrating relevant features was constructed using recently reported transmembrane boundaries (Fig. 1) (Nickerson *et al.*, 2010) and TMRPres2D software (http://bioinformatics.biol.uoa.gr/TMRPres2D). The conserved cholesterol recognition amino acid concensus, CRAC motif (-L/V-(X1-5)-Y-(X1-5)-R/K-), at TERE1 amino acids 100-L(VNTY)Y(DFS)K-109, near the membrane interface carries the strong implication that TERE1 is a cholesterol-binding, storage, or transfer protein similar to other CRAC domain proteins (Epand, 2008). The adjacent aspartate-rich, FARM motif, DDXXXXD, from 117-DDRTLVD-123 is similar to farnesyl diphosphate synthetase (Szkopinska and Plochocka, 2005) and has been referred to as a putative ligand/polyprenyldiphosphate binding site (Weiss *et al.*, 2007). The heme regulatory motif (30-XCPXX-34) and oxidoreductase motif (145-CXXC-148) suggest that TERE1 activity may be affected by cellular redox state (Weiss *et al.*, 2007). The approximate polyclonal antibody binding sites and engineered stop mutations at Y174 and E242 used in this study and the prominent loops 1–3 that contain mutations (in red) associated with SCD are also shown (Weiss *et al.*, 2007; Nickerson *et al.*, 2010). These loops may constitute a binding interface for interacting proteins, APOE and TBL2.

TERE1 expression in invasive bladder cancer

We conducted an immuno-histochemical analysis using a human bladder TMA to examine TERE1 expression in stage T1 papillary carcinoma compared to T2 (and greater) muscle invasive specimens. The representative anti-TERE1 staining levels were sorted into the four groups (low, mild, moderate, and high) based on the assigned labeling index and are depicted in Figure 2. The labeling index for each core was derived by multiplying the percentage of positive cells by an intensity score ranging from 0 to 3+. The average value obtained from three cores was assigned as the score for that particular case. The results of 22 T1 and 56 T2 bladder cancer specimens using the rabbit anti-TERE1 antibody are summarized in Table 1. Almost a third of the >T2 specimens (28.6%) displayed low level TERE1 staining, considered negative, and staining was completely absent in 5/56. For T1

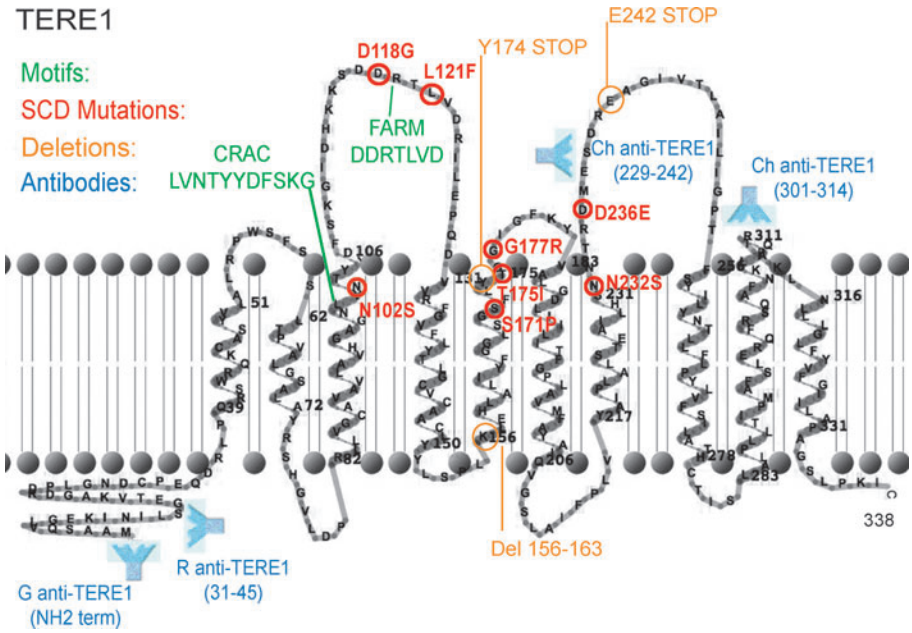

FIG. 1. Diagram of the 338 amino acid TERE1 protein depicting 10 a-helical transmembrane domains, the conserved CRAC and FARM motifs (green), sites of point mutations associated with SCD (red), and positions of engineered STOP codon truncation mutants (orange). Also shown are the antigen regions (blue) for polyclonal antibodies.

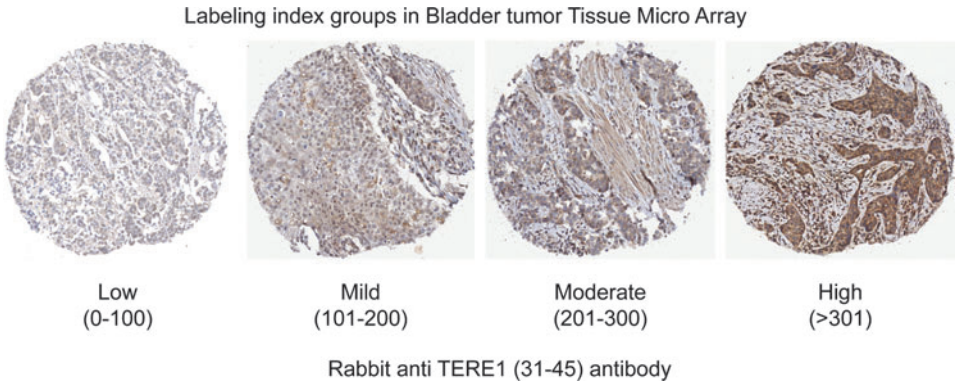

FIG. 2. Immunohistochemical staining of bladder tumor tissue microarray with the rabbit anti-TERE1 (31–45) antibody. Representative labeling index groups (low, mild, moderate, and high) based on intensity of staining *x*% of tumor cells staining (refer Table 1).

specimens, low level staining was observed in only a minority of cases (9.0%) and there were none in which staining was absent. Almost half of the T1 specimens (45.4%) exhibited the high level of TERE1 staining, in contrast to only 25% of the T2 specimens. The average TERE1 labeling indexes of the T1 and >T2 populations were judged by a *t*-test for unequal sample sizes to be significantly different ($p = 0.005$–0.01). Overall, the decrease in the TERE1 protein expression observed here allows us to place an estimate of reduced TERE1 expression in almost a third of cases of invasive transitional cell carcinoma.

TERE1/TBL2 expression in bladder cancer cell lines

We evaluated TERE1 and TBL2 expression in a panel of bladder cell lines. Figure 3A shows a very low level of endogenous TERE1 levels in several bladder cancer cell lines (top) yet conserved expression of TBL2 (bottom), with two different antibodies in each case. Reduced TERE1 expression may be a feature in common among bladder cancer cell lines and some invasive bladder cancer specimens.

TERE1 effects on tumorigenicity

We extended our analysis of TERE1 in bladder cancer to see if TERE1 overexpression may inhibit tumorigenic growth in nude mice. There was a significantly decreased *in vivo* growth of J82-TERE1 cells in nude mice ($p < 0.0005$) (Fig. 3B). Tumors resulting from TERE1-transduced J82 cells (mean tumor size $= 0.13 + 0.03\,cm^3$) were reduced in size by 88% compared to tumors from control vector-transduced J82 cells (mean tumor size $= 1.09 + 0.13\,cm^3$).

Elevation of TERE1 or TBL2 proteins reduces cellular cholesterol levels

We transfected HEK293 cells with expression plasmids for full length and for deletion mutants of TERE1 and TBL2 proteins and confirmed expression in the immunoblots in Figure 4A. The left panel shows TERE1 at its expected ~37 kDa size using an affinity purified Rabbit anti-TERE1 polyclonal antibody. The right panel was probed with Ch anti-TBL2 (353–366) and detects the ~49 kDa TBL2 protein. Next, we measured cholesterol using the well-established Amplex red fluorometric assay relative to a dilution series of cholesterol standards using equal amounts of protein from the transfected cell lysates (Amundson and Zhou, 1999). Oxidation of cholesterol by CO yields H_2O_2, which reacts with the Amplex red reagent to produce the highly fluorescent resorufin dye. Samples with elevated expression of TERE1 or TBL2 proteins had significantly reduced intracellular cholesterol levels compared to control vector (**$p < 0.01$) (Fig. 4B, left panel). We also found that overexpression of the 2/3 length deletion mutants TERE1-E242 STOP and TBL2-E311 STOP caused similar cholesterol reductions (4B, right panel). The 1/3 length TERE1-Y174 STOP and even small deletions in the middle of TERE1-Del (156–163) resulted in partial cholesterol reduction. This suggests the possibility that overexpression of these motifs may be titrating factors affecting cholesterol homeostasis. Cholesterol reduction was abolished with expression of the 1/3 length TBL2-Y174 STOP and the TBL2-Del NLS (184–190) protein with a small deletion in the putative NLS (Fig. 4B, right panel). Both of these mutant TBL2 proteins lose the putative nuclear localization signal. Either the mutant TBL2 proteins may be saturating

Table 1. Analysis of TERE1 Staining and Invasive Status T1 Versus >T2 in Bladder Tumor Tissue Microarray

	LI (range)						
	Low (0–100)	*Mild (101–200)*	*Moderate (201–300)*	*High (≥301)*	*Total*	*Avg. LI*	*SD*
T1: lesion	2/22 (9.0%)	6/22 (27.3%)	4/22 (18.2%)	10/22 (45.5%)	22	231.9	80.5
≥T2: invasive	16/56 (28.6%)	13/56 (23.2%)	11/56 (19.6%)	14/56 (25.0%)	56	169.3	109.8

Representative LI groups (low, mild, moderate, and high) based on intensity of staining *x*% of tumor cells staining. TERE1 expression is reduced in a third of invasive bladder tumor specimens. A significantly greater number of >T2 specimens show low TERE1 staining than T1 ($p = 0.005$–0.01) (refer Fig. 2).

LI, labeling index.

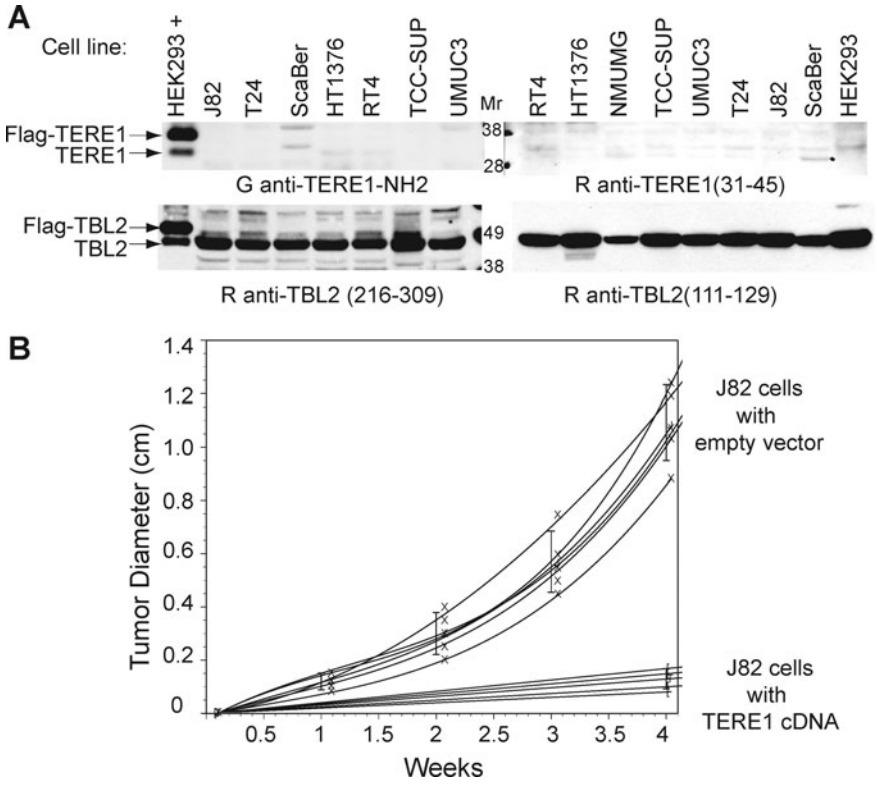

FIG. 3. Expression and tumorigenicity. **(A)** Expression of endogenous TERE1, and TBL2 in human bladder cancer cell lines from ATCC. Equal protein amounts of cell lysates from bladder cancer cell lines indicated in labels were resolved by SDS-PAGE, immunoblotted, and probed with indicated antibodies. HEK293 transfected with Flag-TERE1 or Flag-TBL2 (depicted as HEK293+) served as positive controls for antibodies. **(B)** Tumorigenicity of J82 cells transduced with *TERE1* compared to vector control in nude mice. J82 cells were transduced with the retroviral pTRE empty vector or pTRE-*TERE1*, injected subcutaneously into nude mice, and tumor growth was measured after 30 days. There was a significant decrease *in vivo* growth of J82TERE1 cells in nude mice compared to control transduced cells ($p < 0.0005$).

available TERE1 and/or nuclear localization may be important for cholesterol modulation by TBL2.

To ensure that the observed changes in the Amplex red assay were specific for cholesterol and thus dependent on the presence of the cholesterol-specific enzymes, we performed control evaluations by leaving out the cholesterol-specific enzymes: CE and CO. Virtually all of the changes in cholesterol from lysates infected with Ad-TERE1 depended on the presence of CO in the assay, and there was no appreciable difference when CE was omitted (not shown). In the absence of cholesterol-specific enzymes, the assay can monitor production of H_2O_2 in fresh cell lysates. We found that TERE expression results in an $\sim$3-fold increase in H_2O_2 relative to control vector (not shown). Overall, these results confirm the cholesterol-modulatory potential of both TERE1 and TBL2, and that overexpression can significantly reduce cellular cholesterol levels.

Decreased TERE1 and TBL2 protein levels elevate cellular cholesterol levels

Knockdown technology was used to reduce the endogenous cellular level of the TERE1 and TBL2 proteins. We validated a panel of CMV-driven mammalian miRNA expression plasmids containing EmGFP-miRNA-cassettes targeting six different sequences for *TERE1*, and for *TBL2*. Progressive knock down of the endogenous TERE1 and TBL2 in HEK293 cells was confirmed by expression analysis after transfection of *TERE1* (miRNAs9 and 10) and *TBL2* (miRNAs 3 and 4) relative to the MiR-NC scrambled sequence nonsense control over a period of 36–72 h (Fig. 5A). Significantly, we found 15%–30% increases in cholesterol levels compared to the reference MIR-NC control from cell lysates with reduced endogenous *TERE1* from miRNA numbers 9 and 10 (left) and TBL2 from miRNA numbers 3 and 4 (right) (Fig. 5B). In addition, different vector sets, a pLenti6.3/V5DEST or a pSM2-shRNA-*TERE1* retroviral plasmid, achieved identical results (not shown). Similar cholesterol elevations were also achieved with several different miRNA targeting sequences for both *TERE1* (numbers 7–10) and *TBL2* (numbers 1–6) (not shown); hence, the changes in cholesterol are not likely due to off-target effects.

TERE1 SCD mutations alter cholesterol levels

TERE1's role in cholesterol metabolism, suggested by the APOE interaction (McGarvey *et al.*, 2005), was reinforced by the association of point mutations in *TERE1* with SCD, a corneal cholesterol and lipid accumulation disorder (Weiss *et al.*, 2007). We transfected HEK293 cells with Flag-tagged wild-type and SCD mutant *TERE1* plasmids with point mutations at N102S, D118G, L121F, S171P, T175I, G177R, N232S, D236E, and confirmed equivalent expression levels of the wild-type, mutant, and deletion proteins (Figs. 6A and 4A). Next, we compared the total cholesterol levels in the lysates from cells transfected with the wild-type and mutant TERE1 proteins. The cholesterol levels of transfected SCD TERE1 mutants differed significantly in most cases from wild-type TERE1 and from vector control (Fig. 6B).

TERE1 SCD mutants exhibit reduced binding to APOE

We applied molecular modeling to evaluate the TERE1/APOE interaction. From 20 different docking arrangements one appeared to be of special interest since in this model almost all amino acid residues identified from mutations that

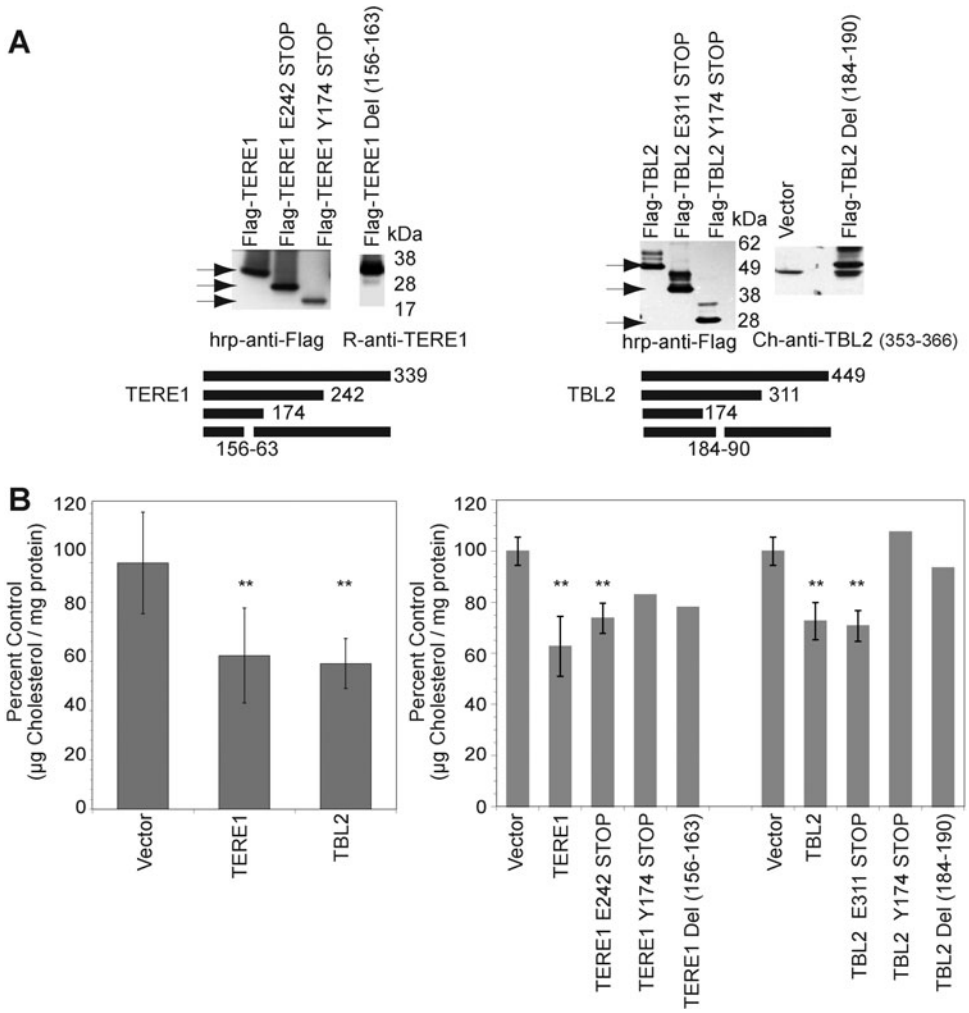

FIG. 4. TERE1 and TBL2 expression result in cholesterol reduction. **(A)** Ectopic expression of TERE1 and TBL2 proteins (full length and deletion mutants) from HEK293 cell lysates by immunoblot analysis. **(B)** Expression of TERE1 or TBL2 results in a reduced level of cellular cholesterol compared to vector control (**$p < 0.01$). Cell lysates were analyzed by Amplex red assay for cholesterol and by BCA for protein.

are critical for causing the SCD are in interaction with APOE. The molecular docking model depicted in Figure 7A shows that the binding is stabilized especially by hydrophobic interactions of L121 (UBIAD1) with V94 (APOE) and the formation of two salt bridges (N118–R39, N236-L50). Next, we tested whether the mutations associated with SCD and simple deletions would affect binding of TERE1 to GST-APOE. The wild-type and mutant test protein lysates of TERE1 prepared from transfected HEK293 cells were tested for binding to equal amounts of purified fusion protein baits: GST-vector and GST-APOE (Fig. 7B; baits not shown). The TERE1 deletion mutant lacking the C-terminal third (E242-STOP) retained strong binding to GST-APOE. Binding to APOE was lost when just the N-terminal third of TERE1 (Y174-STOP) was tested. This maps the interaction with APOE to the middle third of TERE1 (loops 2–3). Further, we demonstrate that some natural point mutations in TERE1 associated with SCD can significantly impair binding to APOE (Fig. 7B). Compared to binding by wild-type TERE1, the TERE1 mutants N102S, D118G, S171P, T175I, and G177R showed reduced binding. This is generally consistent with predictions of the model: especially the predicted TERE1 D118–APOE R39 salt bridge affected by D118G mutation, and the TERE1 D236- APOE K50 salt bridge affected by D236E. Given the role of APOE in cholesterol and lipid recycling, impaired APOE interaction with mutant TERE1 proteins may be a defect that contributes to elevated corneal cholesterol and lipids associated with SCD. By extension, this suggests the possibility that reduced TERE1 expression in invasive bladder cancer might also affect cholesterol and lipid levels.

Cholesterol modulation in bladder cancer cell lines

We examined whether elevation of TERE1 expression in bladder cancer cell lines would affect cellular cholesterol levels. We infected the J82, ScaBer, TCCSUP, HT1376, and UMUC3 cell lines with an adenovirus encoding a TERE1 or a GFP cDNA and compared cellular cholesterol levels. The immunoblots in Figure 8A show exogenous TERE1 expression in the Ad TERE1-infected J82, ScaBer, TCCSUP, HT1376, and UMUC3 cell lines. Figure 8B shows the degree of infectivity assessed by GFP expression and that cholesterol levels are reduced by up to 30% via TERE1 expression in these cell lines. Cholesterol reduction by elevated TERE1 expression appears to be a common response, yet shows some differences in magnitude across several different cell lines, thus may likely be influenced by additional variables in different cell lines.

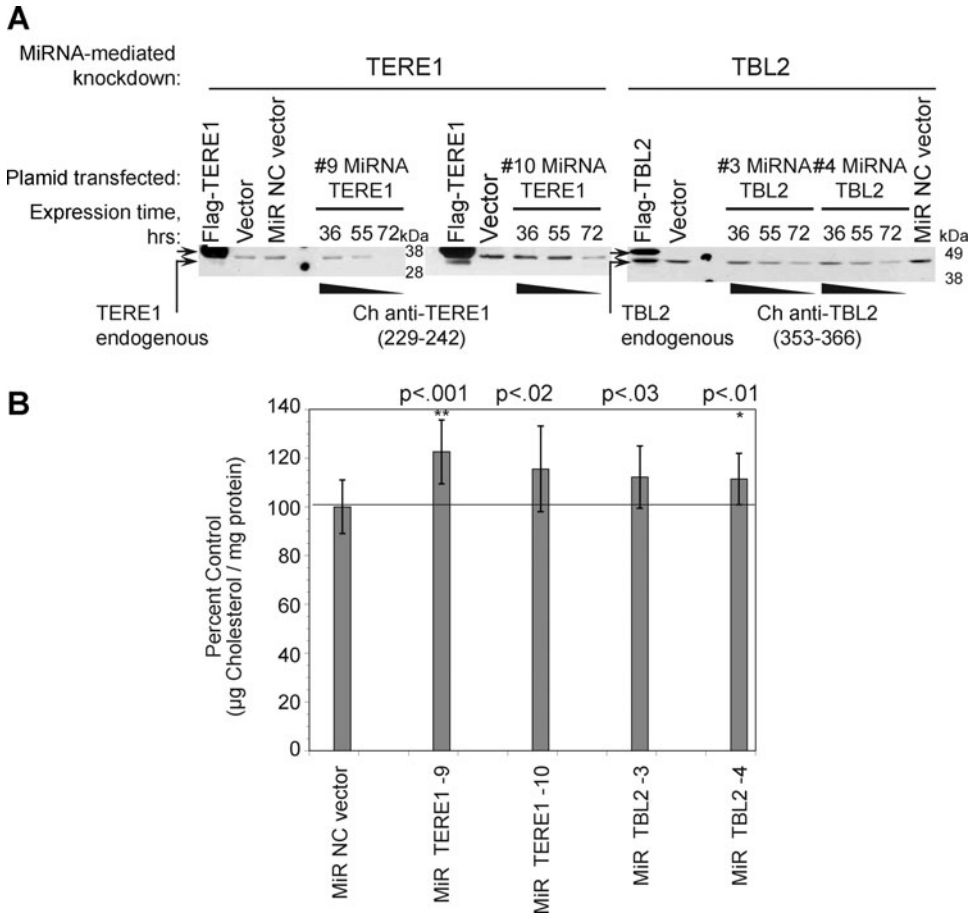

FIG. 5. Knockdown of endogenous TERE1 and TBL2 expression elevates cellular cholesterol. **(A)** Reduced TERE1 and TBL2 expression in HEK293 cells after transfection of miRNA expression plasmids targeting TERE1 (9, 10) and TBL2 (3, 4). Cell lysates were analyzed by immunoblot analysis after 36, 55, and 72 h for endogenous TERE1 and TBL2 expression, protein, and cholesterol content relative to a scrambled miRNA sequence control vector (MiR NC control). **(B)** Cell lysates with reduced TERE1 or TBL2 levels exhibit elevated cholesterol levels relative to MiR NC control vector (**$p < 0.001$, *$p < 0.01$).

Discussion

Loss of TERE1 expression and bladder cancer progression

We have presented evidence that support the hypothesis that a loss of TERE1 may contribute to tumor progression in transitional cell carcinoma of the bladder. The immunohistochemical data show that expression of the TERE1 protein is reduced in a third of invasive human bladder cancer specimens and hence occurs with sufficient frequency to potentially affect a significant number of individuals. The finding that forced expression of TERE1 can dramatically inhibit tumor growth is consistent with the reported inhibitory effects of vitamin K-2 and K-3 on tumor cells and the vitamin K-2 synthetic activity of TERE1 that produces K-3 as an intermediate (Lamson and Plaza, 2003; Jamison *et al.*, 2004; Azuma *et al.*, 2009; Gilloteaux *et al.*, 2010; Lamson *et al.*, 2010; Nakagawa *et al.*, 2010). We did observe an increase in H_2O_2 in fresh lysates from Ad-TERE1-infected J82 cells consistent with TERE1-mediated synthesis of vitamins K-2 or K-3. Both vitamin K-2 and K-3 are redox-cycling and alkylating quinones known to generate oxidative stress (superoxide and H_2O_2), alkylate thiols and amines (O'Brien, 1991) and lead to different types of growth inhibition, autoschizis, necrosis, or apoptosis (Lamson and Plaza, 2003; Shibayama-Imazu *et al.*, 2006; Jamison *et al.*, 2010). This also suggests the possibility that TERE1 expression may be an oxidative stress liability that is selected against during tumor cell metabolic reprogramming to the invasive phenotype.

Cholesterol homeostasis overview

Cellular cholesterol levels are normally highly regulated via a complex interplay between several processes: transport (influx and efflux), *de novo* synthesis, trafficking, storage, and recycling (Goldstein *et al.*, 2006; Ikonen, 2008; Raghow *et al.*, 2008). In general, the SREBP transcriptional regulator proteins activate genes for cholesterol synthesis and influx, and the Liver X Receptor, (LXR) nuclear receptors activate cholesterol efflux; however, both also regulate different aspects of fatty acid metabolism (Abildayeva *et al.*, 2006; Wang *et al.*, 2008b; Raychaudhuri and Prinz, 2010). LXR pathways activate the apo-protein carriers such as APOAI, APOE, and the transporters such as the ATP binding cassette proteins ABC-A1, -G1, -G4, and SRBI, through which efflux proceeds to mature High density Lipoprotein, (HDL) (Tall, 2008; Zhou *et al.*, 2010). LXR targets can be activated by oxysterols derived from the cholesterol pathway, by fatty acids, or by cross regulation from other nuclear receptors such as the steroid and xenobiotic receptor, SXR (Abildayeva *et al.*, 2006; Tamehiro *et al.*, 2007; Wang *et al.*, 2008b; Zhou *et al.*, 2009). The multiple ways these networks may be dysregulated in the context of tumor cell metabolic reprogramming are not clearly defined.

Cholesterol as a determinant of progression

Elevated intracellular tumor cholesterol is becoming recognized as a general mechanism of tumor progression in prostate and several other cancers and a number of diverse

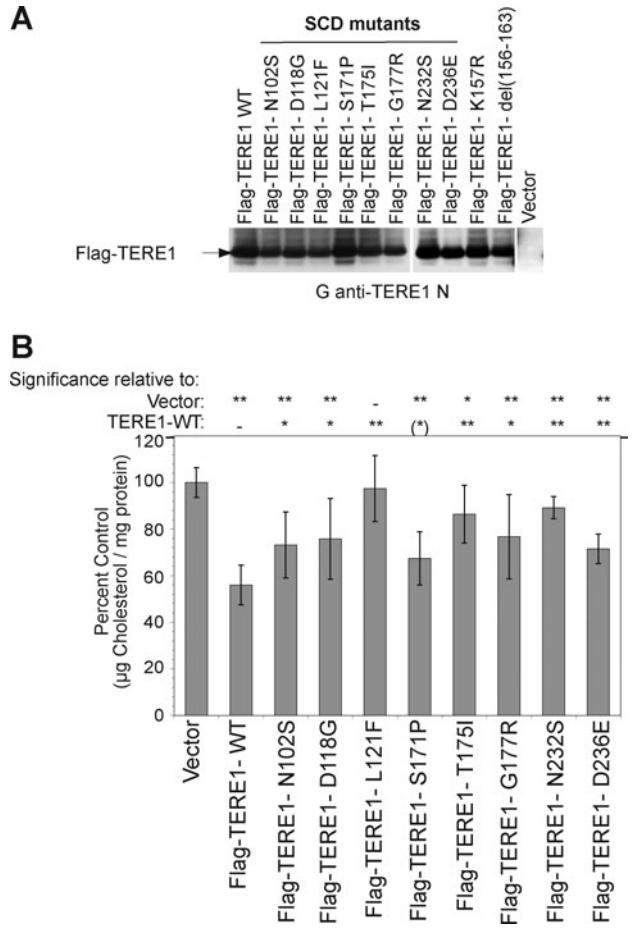

FIG. 6. Natural mutations in *TERE1* associated with Schnyder's corneal dystrophy (SCD) alter the cholesterol levels relative to wild type. **(A)** HEK293 cell lysates expressing ectopic Flag-TERE1 proteins bearing point mutations associated with SCD exhibit similar expression levels. Detection by goat anti-TERE1-NH2 immunoblots. **(B)** Cell lysates were analyzed for total cholesterol 72 h after transfection. In spite of similar expression levels in **(A)**, cholesterol levels of mutants differ compared to wild type and to vector control [$^{**}p < 0.001$, $^{*}p < 0.01$, $^{(*)}p < 0.05$].

mechanisms continue to be defined (Swinnen *et al.*, 2006; Di Vizio *et al.*, 2008; Patra, 2008; Batarseh and Papadopoulos, 2010; Twiddy *et al.*, 2010). Important growth-signaling complexes for pathways such as TGFβ, EGFR/MAPK/ERK, AKT, and the AR reside within cholesterol-rich microdomains referred to as lipid rafts whose signaling integrity can be modulated by changes in cellular cholesterol levels that affect membrane fluidity, transport, and protein complex assembly and stability (Adam *et al.*, 2007; Freeman *et al.*, 2007; Montero *et al.*, 2008). Elevated mitochondrial cholesterol associated with different cancers has also been demonstrated to impair the BAX-mediated apoptotic permeability pore associated with apoptosis and provide an apoptotic escape mechanism (Zhuang *et al.*, 2005; Li *et al.*, 2006, 2008; Martinez-Abundis *et al.*, 2007; Oh *et al.*, 2007; Christenson *et al.*, 2008).

TERE1 modulation of cholesterol

Our studies show that the TERE1 protein is a novel component of the dynamic cellular cholesterol regulatory network. Ectopic TERE1 overexpression reduces cholesterol and miRNA-mediated knockdown raises cholesterol. The role of TERE1 in vitamin K-2, menaquinone, synthesis (Nakagawa *et al.*, 2010) provides a highly probable and established mechanism of TERE1-mediated cholesterol modulation. Menaquinone is a known ligand for the nuclear receptor SXR (Tabb *et al.*, 2003; Shearer and Newman, 2008; Zhou *et al.*, 2009). SXR is known to heterodimerize with RXR and cross regulate LXR target genes that have well-established roles in modulation of cellular cholesterol efflux (Landes *et al.*, 2003; Sonoda *et al.*, 2005; Wang and Rader, 2007; Wang *et al.*, 2007, 2008b; Lim and Huang, 2008; Brown and Jessup, 2009; Zhou *et al.*, 2009). Elevation of TERE1 would be predicted to increase cholesterol efflux and reduce cell cholesterol, consistent with our observations.

We also found that ectopic expression of several SCD point mutant TERE1 proteins in the HEK293 cell line resulted in altered cell cholesterol relative to wild-type TERE1 and control vector. A previous study compared lymphocyte populations isolated from normal and SCD patients after immortalization by EBV and found no differences in cell cholesterol levels (Nickerson *et al.*, 2010). The apparent discrepancy may be due to the many differences between the two studies. First, the two studies examined different sets of TERE1 mutations: A97T and V122E TERE1 mutations in lymphocytes and the N102S D118G, L121F, S171P, T175I, G177R, N232S, and D236E mutations studied here. Also, the exogenous expression approach of this study in HEK293 or bladder cancer cells may amplify the cholesterol effect. The lymphocytes with normal or mutant endogenous TERE1 may favor other mechanisms to compensate and maintain cholesterol homeostasis, in contrast to transfected HEK293 cells and possibly natural corneal SCD cells. Overall, the detailed mechanism of TERE1 is not fully understood, but likely involves several steps based on vitamin K metabolism, oxidative stress, and mobilization of cholesterol efflux. The abundance and activity of components responsible for these processes may vary in different cell types and possible cell-type-specific influences will need to be addressed in future studies.

TBL2 modulation of cholesterol

We have also shown that the TERE1-interacting protein, TBL2, can modulate cellular cholesterol. Ectopic TBL2 overexpression reduces cholesterol and miRNA-mediated knockdown raises cholesterol. TBL2 is also considered a candidate disease gene associated with triglyceride metabolism, but its role is unknown (Wang *et al.*, 2008a). Phosphorylation of TBL2 by ATM/ATM in response to DNA damage identifies TBL2 as a member of the cellular oxidative damage response network (Matsuoka *et al.*, 2007). TBL2 was also recently identified as a PDK1-interacting protein by mass spectroscopic analysis after PDK1 immunoprecipitation (Behrends *et al.*, 2010). The mechanism of TBL2 in modulation of cellular cholesterol is presently undefined, however; by virtue of its association with TERE1, which leads to synthesis of vitamin K-2, a role in metabolic redox signaling should be explored.

Implications of TERE1 protein interactions with APOE

The role of TERE1 in vitamin K metabolism fits well with the TERE1 interaction with APOE (McGarvey *et al.*, 2001, 2003). Both cholesterol and vitamin K homeostasis use

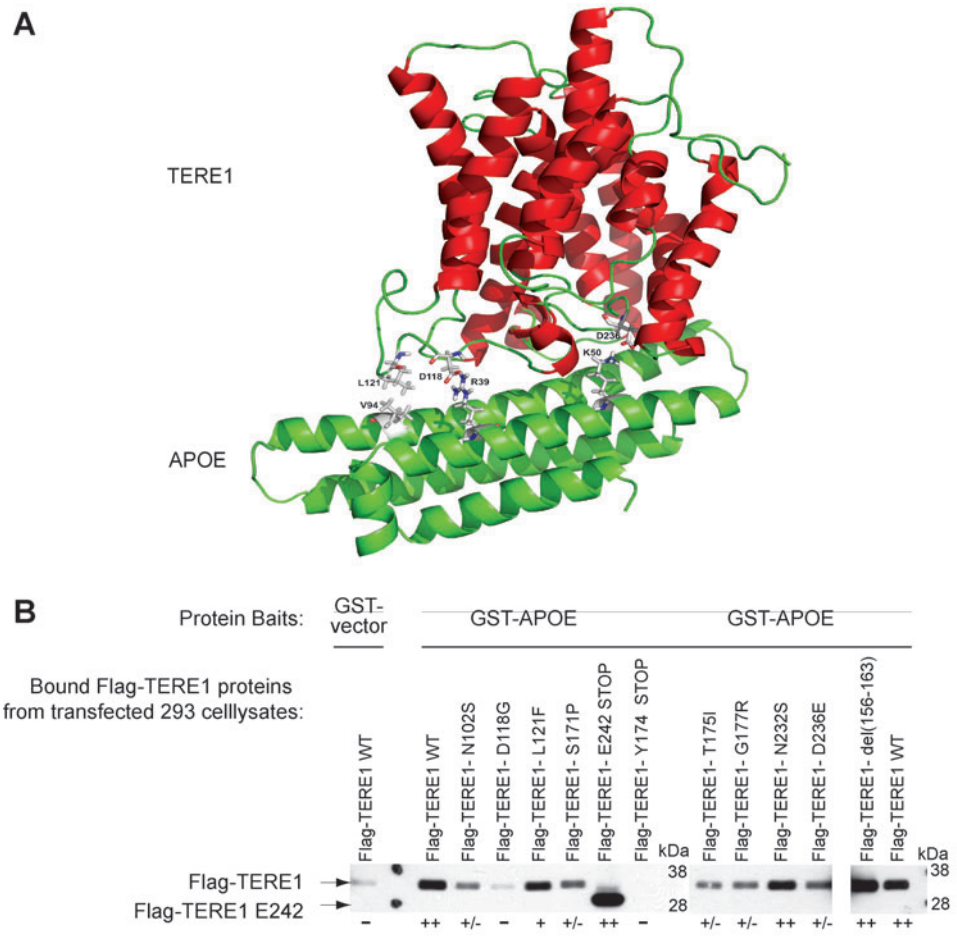

FIG. 7. Mutations in TERE1 affect binding to GST-APOE. **(A)** Molecular docking model for TERE1 and APOE proteins. **(B)** Flag-TERE1 test protein lysates, as in Figure 6A, were tested for binding to full-length GST-APOE. Binding was detected by immunoblotting with hrp-labeled anti-FLAG M2 antibody. SL refers to straight lysates. (++) Strong binding, (+/−) reduced binding, and (−) loss of binding.

overlapping mechanisms of the APOE, LXR target gene. APOE transports cholesterol and can also bind and transport vitamin K (Lamon-Fava *et al.*, 1998; Otsuka *et al.*, 2005; Shearer and Newman, 2008). As a ligand for SXR, vitamin K-2 can activate LXR targets such as APOE and the ABC transporters that efflux vitamin K and cholesterol (Shukla *et al.*, 2007; Chisaki *et al.*, 2009). Pharmacological application of vitamins K-2 and K-3 are also linked to oxidative stress (Gilloteaux *et al.*, 2006; Shibayama-Imazu *et al.*, 2006; Shearer and Newman, 2008; Amalia *et al.*, 2010). APOE is believed to play a role in oxysterol-induced efflux as part of a lipoprotein-mediated defense against oxidative stress (Laffitte *et al.*, 2001; Landes *et al.*, 2003; Carter, 2007; Rezen *et al.*, 2010). Thus, efflux can be viewed as a mechanism to relieve the oxidative stress of excess cholesterol and oxysterols (Galea and Brown, 2009). In this regard, mutations in TERE1 that reduce APOE binding may impair cholesterol and lipid recycling by APOE, and lead to elevated intracellular cholesterol via reduced efflux (Prack *et al.*, 1994; Heeren *et al.*, 2004; Abildayeva *et al.*, 2006; Ha *et al.*, 2009). It may also raise basal oxidative stress, consistent with recent reports regarding pathogenesis of SCD and other corneal dystrophies (Gatzioufas *et al.*, 2010; Jurkunas *et al.*, 2010).

Concluding Remarks

Current views on tumor cell metabolism (the reverse Warburg hypothesis) emphasize the role oxidative stress plays in malignant progression to drive genomic instability, mitogenic signaling, motility, inflammation, and angiogenesis (Behrend *et al.*, 2003; Pavlides *et al.*, 2010; Ralph *et al.*, 2010; Sone *et al.*, 2010). Evidence links oxidative stress to the invasive phenotype in breast and pancreatic cancer (Silva *et al.*, 2003; Brown and Jessup, 2009; Ishikawa *et al.*, 2010). An inherent corollary to oxidative stress relates to its tolerance and the potentially heightened vulnerability of tumor cells to further increases in ROS levels (Pani *et al.*, 2010). Tumor progression depends on adaptations to maintain an elevated oxidative stress level; however, tumor cells must manage oxidative stress levels below the apoptotic threshold. In this regard, subversion of apoptotic signaling by elevated mitochondrial cholesterol is highly relevant (Montero *et al.*, 2008; Garcia-Ruiz *et al.*, 2009). The natural TERE1-mediated targeting of vitamin K-2 synthesis to mitochondria may represent a form of oxidative stress liability to tumor cell metabolism during progression to invasion. This idea is supported by reports of induction of mitochondrial damage, autozchizis, autophagy, and/or apoptosis and the inhibition of many different types of tumor cell lines after vitamin K-2 and K-3 treatments (Lamson and Plaza, 2003; Jamison *et al.*, 2004; Azuma *et al.*, 2009; Gilloteaux *et al.*, 2010). Menadione was recently approved by the FDA in combination with vitamin C (Apatone), for clinical trials for cancer therapy of inoperable bladder cancers stages III and IV (Ralph *et al.*, 2010). This also suggests that a reduced TERE1 status might be a relevant marker to identify Apatone-sensitive patients.

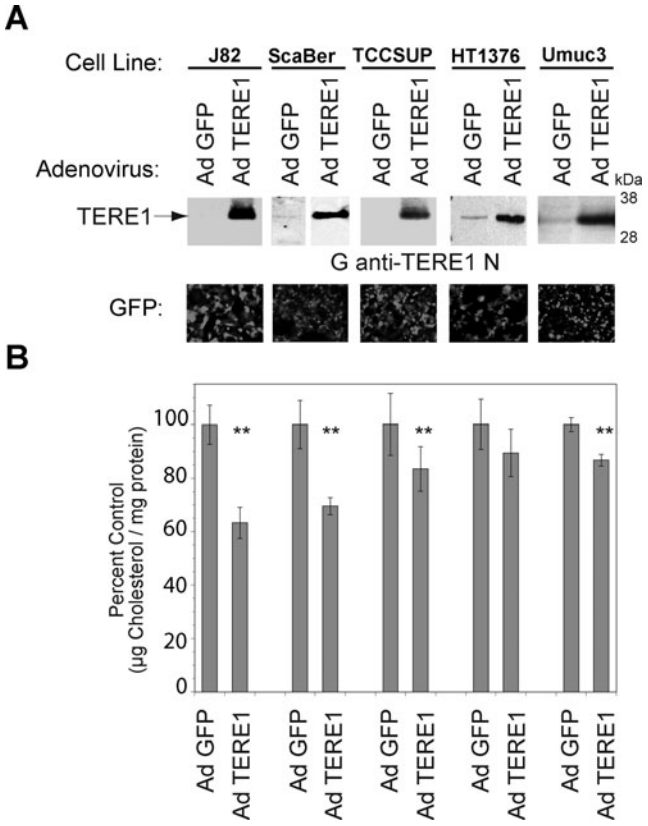

FIG. 8. Expression of TERE1 adenovirus in bladder cancer cell lines reduces cellular cholesterol levels. **(A)** TERE1 expression levels in human bladder cancer cell lines J82, ScaBer, TCCSUP, HT1376, and UMUC-3 after infection with Adenovirus encoding *TERE1* or *GFP* vector. **(B)** AdCMV-*TERE1* expression reduces cellular cholesterol relative to AdCMV-*GFP* vector control (**$p < 0.001$). GFP shown as an indicator of infectivity. Cell lysates were analyzed for protein and cholesterol content 3 days postinfection.

The loss of TERE1 expression may be a defect in mitochondrial to nuclear SXR signaling that tumors use to uncouple vitamin K-mediated oxidative stress signaling in mitochondria from apoptosis or negative growth signaling by elevation of cholesterol.

Acknowledgments

We thank the Veterans Affairs Merit Review and the Veterans Affairs Medical Center Philadelphia for the grant support to S.B. Malkowicz. We thank the Innisfree Foundation of Bryn Mawr, PA, and The Castleman Family Fund for their generous support to S.B. Malkowicz and W.J. Fredericks.

Disclosure statement

No competing financial interests exist.

References

Abildayeva, K., Jansen, P.J., Hirsch-Reinshagen, V., Bloks, V.W., Bakker, A.H., Ramaekers, F.C., *et al.* (2006). 24(S)-hydroxycholesterol participates in a liver X receptor-controlled pathway in astrocytes that regulates apolipoprotein E-mediated cholesterol efflux. J Biol Chem **281,** 12799–12808.

American Cancer Society (ACS). (2010). *Cancer Facts and Figures 2010* (Atlanta, GA). Available at http://www.cancer.org/acs/groups/content/@epidemiologysurveilance/documents/document/acspc-026238.pdf

Adam, R.M., Mukhopadhyay, N.K., Kim, J., Di Vizio, D., Cinar, B., Boucher, K., *et al.* (2007). Cholesterol sensitivity of endogenous and myristoylated Akt. Cancer Res **67,** 6238–6246.

Amalia, H., Sasaki, R., Suzuki, Y., Demizu, Y., Bito, T., Nishimura, H., *et al.* (2010). Vitamin K2-derived compounds induce growth inhibition in radioresistant cancer cells. Kobe J Med Sci **56,** E38–E49.

Amundson, D.M., and Zhou, M. (1999). Fluorometric method for the enzymatic determination of cholesterol. J Biochem Biophys Methods **38,** 43–52.

Azuma, K., Urano, T., Ouchi, Y., and Inoue, S. (2009). Vitamin K2 suppresses proliferation and motility of hepatocellular carcinoma cells by activating steroid and xenobiotic receptor. Endocr J **56,** 843–849.

Bandyopadhyay, P.K. (2008). Vitamin K-dependent gamma-glutamylcarboxylation: an ancient posttranslational modification. Vitam Horm **78,** 157–184.

Barrios-Rodiles, M., Brown, K.R., Ozdamar, B., Bose, R., Liu, Z., Donovan, R.S., *et al.* (2005). High-throughput mapping of a dynamic signaling network in mammalian cells. Science **307,** 1621–1625.

Baruthio, F., Quadroni, M., Ruegg, C., and Mariotti, A. (2008). Proteomic analysis of membrane rafts of melanoma cells identifies protein patterns characteristic of the tumor progression stage. Proteomics **8,** 4733–4747.

Batarseh, A., and Papadopoulos, V. (2010). Regulation of translocator protein 18 kDa (TSPO) expression in health and disease states. Mol Cell Endocrinol **327,** 1–12.

Behrend, L., Henderson, G., and Zwacka, R.M. (2003). Reactive oxygen species in oncogenic transformation. Biochem Soc Trans **31,** 1441–1444.

Behrends, C., Sowa, M.E., Gygi, S.P., and Harper, J.W. (2010). Network organization of the human autophagy system. Nature **466,** 68–76.

Bellidomartin, L., and Defrutos, P. (2008). Vitamin K-dependent actions of Gas6. Vitam Horm **78,** 185–209.

Bräuer, L., Brandt, W., Schulze, D., Zakharova, S., Wessjohann, L. (2008). A structural model of the membrane bound aromatic prenyltransferase UbiA from E. coli. Chembiochem 9, 982–92.

Brown, A.J., and Jessup, W. (2009). Oxysterols: sources, cellular storage and metabolism, and new insights into their roles in cholesterol homeostasis. Mol Aspects Med **30,** 111–122.

Bugel, S. (2008). Vitamin K and bone health in adult humans. Vitam Horm **78,** 393–416.

Carter, C.J. (2007). Convergence of genes implicated in Alzheimer's disease on the cerebral cholesterol shuttle: APP, cholesterol, lipoproteins, and atherosclerosis. Neurochem Int **50,** 12–38.

Chisaki, I., Kobayashi, M., Itagaki, S., Hirano, T., and Iseki, K. (2009). Liver X receptor regulates expression of MRP2 but not that of MDR1 and BCRP in the liver. Biochim Biophys Acta **1788,** 2396–2403.

Christenson, E., Merlin, S., Saito, M., and Schlesinger, P. (2008). Cholesterol effects on BAX pore activation. J Mol Biol **381,** 1168–1183.

Comeau, S.R., Gatchell, D.W., Vajda, S., and Camacho, C.J. (2004a). ClusPro: a fully automated algorithm for protein-protein docking. Nucleic Acids Res **32,** W96–W99.

Comeau, S.R., Gatchell, D.W., Vajda, S., and Camacho, C.J. (2004b). ClusPro: an automated docking and discrimination method for the prediction of protein complexes. Bioinformatics **20,** 45–50.

Di Vizio, D., Solomon, K.R., and Freeman, M.R. (2008). Cholesterol and cholesterol-rich membranes in prostate cancer: an update. Tumori **94,** 633–639.

Epand, R.M. (2008). Proteins and cholesterol-rich domains. Biochim Biophys Acta **1778,** 1576–1582.

Freeman, M.R., Cinar, B., Kim, J., Mukhopadhyay, N.K., Di Vizio, D., Adam, R.M., *et al.* (2007). Transit of hormonal and EGF receptor-dependent signals through cholesterol-rich membranes. Steroids **72,** 210–217.

Galea, A.M., and Brown, A.J. (2009). Special relationship between sterols and oxygen: were sterols an adaptation to aerobic life? Free Radic Biol Med **47,** 880–889.

Garcia-Ruiz, C., Mari, M., Colell, A., Morales, A., Caballero, F., Montero, J., *et al.* (2009). Mitochondrial cholesterol in health and disease. Histol Histopathol **24,** 117–132.

Gatzioufas, Z., Charalambous, P., Loew, U., Kozobolis, V., Schirra, F., Krause, M., *et al.* (2010). Evidence of oxidative stress in Schnyder corneal dystrophy. Br J Ophthalmol **94,** 1262–1264.

Gilloteaux, J., Jamison, J.M., Arnold, D., Neal, D.R., and Summers, J.L. (2006). Morphology and DNA degeneration during autoschizic cell death in bladder carcinoma T24 cells induced by ascorbate and menadione treatment. Anat Rec A Discov Mol Cell Evol Biol **288,** 58–83.

Gilloteaux, J., Jamison, J.M., Neal, D.R., Loukas, M., Doberzstyn, T., and Summers, J.L. (2010). Cell damage and death by autoschizis in human bladder (RT4) carcinoma cells resulting from treatment with ascorbate and menadione. Ultrastruct Pathol **34,** 140–160.

Goldstein, J.L., DeBose-Boyd, R.A., and Brown, M.S. (2006). Protein sensors for membrane sterols. Cell **124,** 35–46.

Ha, S.A., Shin, S.M., Kim, H.K., Kim, S., Namkoong, H., Lee, Y.S., *et al.* (2009). Dual action of apolipoprotein E-interacting HCCR-1 oncoprotein and its implication for breast cancer and obesity. J Cell Mol Med **9B,** 3868–75.

Heeren, J., Grewal, T., Laatsch, A., Becker, N., Rinninger, F., Rye, K.A., *et al.* (2004). Impaired recycling of apolipoprotein E4 is associated with intracellular cholesterol accumulation. J Biol Chem **279,** 55483–55492.

Ikonen, E. (2008). Cellular cholesterol trafficking and compartmentalization. Nat Rev Mol Cell Biol **9,** 125–138.

Ishikawa, S., Nagai, Y., Masuda, T., Koga, Y., Nakamura, T., Imamura, Y., *et al.* (2010). The role of oxysterol binding protein-related protein 5 in pancreatic cancer. Cancer Sci **101,** 898–905.

Jamison, J.M., Gilloteaux, J., Nassiri, M.R., Venugopal, M., Neal, D.R., and Summers, J.L. (2004). Cell cycle arrest and autoschizis in a human bladder carcinoma cell line following Vitamin C and Vitamin K3 treatment. Biochem Pharmacol **67,** 337–351.

Jamison, J.M., Gilloteaux, J., Perlaky, L., Thiry, M., Smetana, K., Neal, D., *et al.* (2010). Nucleolar changes and fibrillarin redistribution following apatone treatment of human bladder carcinoma cells. J Histochem Cytochem **58,** 635–651.

Jurkunas, U.V., Bitar, M.S., Funaki, T., and Azizi, B. (2010). Evidence of oxidative stress in the pathogenesis of fuchs endothelial corneal dystrophy. Am J Pathol **177,** 2278–2289.

Kathiresan, S., Melander, O., Guiducci, C., Surti, A., Burtt, N.P., Rieder, M.J., *et al.* (2008). Six new loci associated with blood low-density lipoprotein cholesterol, high-density lipoprotein cholesterol or triglycerides in humans. Nat Genet **40,** 189–197.

Laffitte, B.A., Repa, J.J., Joseph, S.B., Wilpitz, D.C., Kast, H.R., Mangelsdorf, D.J., *et al.* (2001). LXRs control lipid-inducible expression of the apolipoprotein E gene in macrophages and adipocytes. Proc Natl Acad Sci USA **98,** 507–512.

Lamon-Fava, S., Sadowski, J.A., Davidson, K.W., O'Brien, M.E., McNamara, J.R., and Schaefer, E.J. (1998). Plasma lipoproteins as carriers of phylloquinone (vitamin K1) in humans. Am J Clin Nutr **67,** 1226–1231.

Lamson, D.W., Gu, Y.H., Plaza, S.M., Brignall, M.S., Brinton, C.A., and Sadlon, A.E. (2010). The vitamin C: vitamin K3 system—enhancers and inhibitors of the anticancer effect. Altern Med Rev **15,** 345–351.

Lamson, D.W., and Plaza, S.M. (2003). The anticancer effects of vitamin K. Altern Med Rev **8,** 303–318.

Landes, N., Birringer, M., and Brigelius-Flohe, R. (2003). Homologous metabolic and gene activating routes for vitamins E and K. Mol Aspects Med **24,** 337–344.

Li, C.G., Gruidl, M., Eschrich, S., McCarthy, S., Wang, H.G., and Alexandrow, M.G., *et al.* (2008). Insig2 is associated with colon tumorigenesis and inhibits Bax-mediated apoptosis. Int J Cancer **123,** 273–282.

Li, Y.C., Park, M.J., Ye, S.K., Kim, C.W., and Kim, Y.N. (2006). Elevated levels of cholesterol-rich lipid rafts in cancer cells are correlated with apoptosis sensitivity induced by cholesterol-depleting agents. Am J Pathol **168,** 1107–1118; quiz 1404–1405.

Lim, Y.P., and Huang, J.D. (2008). Interplay of pregnane X receptor with other nuclear receptors on gene regulation. Drug Metab Pharmacokinet **23,** 14–21.

Martinez-Abundis, E., Garcia, N., Correa, F., Franco, M., and Zazueta, C. (2007). Changes in specific lipids regulate BAX-induced mitochondrial permeability transition. FEBS J **274,** 6500–6510.

Matsuoka, S., Ballif, B.A., Smogorzewska, A., McDonald, E.R., Hurov, K.E., Luo, J., *et al.* (2007). ATM and ATR substrate analysis reveals extensive protein networks responsive to DNA damage. Science **316,** 1160–1166.

McGarvey, T.W., Nguyen, T., Puthiyaveettil, R., Tomaszewski, J.E., and Malkowicz, S.B. (2003). TERE1, a novel gene affecting growth regulation in prostate carcinoma. Prostate **54,** 144–155.

McGarvey, T.W., Nguyen, T., Tomaszewski, J.E., Monson, F.C., and Malkowicz, S.B. (2001). Isolation and characterization of the TERE1 gene, a gene down-regulated in transitional cell carcinoma of the bladder. Oncogene **20,** 1042–1051.

McGarvey, T.W., Nguyen, T.B., and Malkowicz, S.B. (2005). An interaction between apolipoprotein E and TERE1 with a possible association with bladder tumor formation. J Cell Biochem **95,** 419–428.

Merli, G., and Fink, J. (2008). Vitamin K and thrombosis. Vitam Horm **78,** 265–279.

Montero, J., Morales, A., Llacuna, L., Lluis, J.M., Terrones, O., Basanez, G., *et al.* (2008). Mitochondrial cholesterol contributes to chemotherapy resistance in hepatocellular carcinoma. Cancer Res **68,** 5246–5256.

Nakagawa, K., Hirota, Y., Sawada, N., Yuge, N., Watanabe, M., Uchino, Y., *et al.* (2010). Identification of UBIAD1 as a novel

human menaquinone-4 biosynthetic enzyme. Nature **468,** 117–121.

Nickerson, M.L., Kostiha, B.N., Brandt, W., Fredericks, W., Xu, K.P., Yu, F.S., *et al.* (2010). UBIAD1 mutation alters a mitochondrial prenyltransferase to cause Schnyder corneal dystrophy. PLoS One **5,** e10760.

Nishikawa, Y., Wang, Z., Kerns, J., Wilcox, C.S., and Carr, B.I. (1999). Inhibition of hepatoma cell growth *in vitro* by arylating and non-arylating K vitamin analogs. Significance of protein tyrosine phosphatase inhibition. J Biol Chem **274,** 34803–34810.

O'Brien, P.J. (1991). Molecular mechanisms of quinone cytotoxicity. Chem Biol Interact **80,** 1–41.

Oh, H.Y., Lee, E.J., Yoon, S., Chung, B.H., Cho, K.S., and Hong, S.J. (2007). Cholesterol level of lipid raft microdomains regulates apoptotic cell death in prostate cancer cells through EGFR-mediated Akt and ERK signal transduction. Prostate **67,** 1061–1069.

Otsuka, M., Kato, N., Ichimura, T., Abe, S., Tanaka, Y., Taniguchi, H., *et al.* (2005). Vitamin K2 binds 17beta-hydroxysteroid dehydrogenase 4 and modulates estrogen metabolism. Life Sci **76,** 2473–2482.

Pani, G., Galeotti, T., and Chiarugi, P. (2010). Metastasis: cancer cell's escape from oxidative stress. Cancer Metastasis Rev **29,** 351–378.

Patra, S.K. (2008). Dissecting lipid raft facilitated cell signaling pathways in cancer. Biochim Biophys Acta **1785,** 182–206.

Pavlides, S., Tsirigos, A., Vera, I., Flomenberg, N., Frank, P.G., Casimiro, M.C., *et al.* (2010). Loss of stromal caveolin-1 leads to oxidative stress, mimics hypoxia and drives inflammation in the tumor microenvironment, conferring the "reverse Warburg effect": a transcriptional informatics analysis with validation. Cell Cycle **9,** 2201–2219.

Perez Jurado, L.A., Wang, Y.K., Francke, U., and Cruces, J. (1999). TBL2, a novel transducin family member in the WBS deletion: characterization of the complete sequence, genomic structure, transcriptional variants and the mouse ortholog. Cytogenet Cell Genet **86,** 277–284.

Prack, M.M., Rothblat, G.H., Erickson, S.K., Reyland, M.E., and Williams, D.L. (1994). Apolipoprotein E expression in Y1 adrenal cells is associated with increased intracellular cholesterol content and reduced free cholesterol efflux. Biochemistry **33,** 5049–5055.

Raghow, R., Yellaturu, C., Deng, X., Park, E., and Elam, M. (2008). SREBPs: the crossroads of physiological and pathological lipid homeostasis. Trends Endocrinol Metab **19,** 65–73.

Ralph, S.J., Rodriguez-Enriquez, S., Neuzil, J., Saavedra, E., and Moreno-Sanchez, R. (2010). The causes of cancer revisited: "mitochondrial malignancy" and ROS-induced oncogenic transformation—why mitochondria are targets for cancer therapy. Mol Aspects Med **31,** 145–170.

Raychaudhuri, S., and Prinz, W.A. (2010). The diverse functions of oxysterol-binding proteins. Annu Rev Cell Dev Biol **26,** 157–177.

Rezen, T., Rozman, D., Pascussi, J.M., and Monostory, K. (2010). Interplay between cholesterol and drug metabolism. Biochim Biophys Acta **1814,** 146–160.

Ryan, R.F., Schultz, D.C., Ayyanathan, K., Singh, P.B., Friedman, J.R., Fredericks, W.J., *et al.* (1999). KAP-1 corepressor protein interacts and colocalizes with heterochromatic and euchromatic HP1 proteins: a potential role for Kruppel-associated box-zinc finger proteins in heterochromatin-mediated gene silencing. Mol Cell Biol **19,** 4366–4378.

Sanchez-Carbayo, M., and Cordon-Cardo, C. (2007). Molecular alterations associated with bladder cancer progression. Semin Oncol **34,** 75–84.

Schabath, H., Runz, S., Joumaa, S., and Altevogt, P. (2006). CD24 affects CXCR4 function in pre-B lymphocytes and breast carcinoma cells. J Cell Sci **119,** 314–325.

Shearer, M.J., and Newman P. (2008). Metabolism and cell biology of vitamin K. Thromb Haemost **100,** 530–547.

Shibayama-Imazu, T., Sonoda, I., Sakairi, S., Aiuchi, T., Ann, W.W., Nakajo, S., *et al.* (2006). Production of superoxide and dissipation of mitochondrial transmembrane potential by vitamin K2 trigger apoptosis in human ovarian cancer TYK-nu cells. Apoptosis **11,** 1535–1543.

Shukla, S., Wu, C.P., Nandigama, K., and Ambudkar, S.V. (2007). The naphthoquinones, vitamin K3 and its structural analogue plumbagin, are substrates of the multidrug resistance linked ATP binding cassette drug transporter ABCG2. Mol Cancer Ther **6,** 3279–3286.

Silva, J., Beckedorf, A., and Bieberich, E. (2003). Osteoblast-derived oxysterol is a migration-inducing factor for human breast cancer cells. J Biol Chem **278,** 25376–25385.

Sone, H., Akanuma, H., and Fukuda, T. (2010). Oxygenomics in environmental stress. Redox Rep **15,** 98–114.

Sonoda, J., Chong, L.W., Downes, M., Barish, G.D., Coulter, S., Liddle, C., *et al.* (2005). Pregnane X receptor prevents hepatorenal toxicity from cholesterol metabolites. Proc Natl Acad Sci USA **102,** 2198–2203.

Suvarna, K., Stevenson, D., Meganathan, R., Hudspeth, M.E. Menaquinone (vitamin K2) biosynthesis: localization and characterization of menA gene from Escherichiacoli. (1998) J Bacteriol **180,** 2782–7.

Swinnen, J.V., Brusselmans, K., and Verhoeven, G. (2006). Increased lipogenesis in cancer cells: new players, novel targets. Curr Opin Clin Nutr Metab Care **9,** 358–365.

Szkopinska, A., and Plochocka, D. (2005). Farnesyl diphosphate synthase; regulation of product specificity. Acta Biochim Pol **52,** 45–55.

Tabb, M.M., Sun, A., Zhou, C., Grun, F., Errandi, J., Romero, K., *et al.* (2003). Vitamin K2 regulation of bone homeostasis is mediated by the steroid and xenobiotic receptor SXR. J Biol Chem **278,** 43919–43927.

Tall, A.R. (2008). Cholesterol efflux pathways and other potential mechanisms involved in the athero-protective effect of high density lipoproteins. J Intern Med **263,** 256–273.

Tamehiro, N., Shigemoto-Mogami, Y., Kakeya, T., Okuhira, K., Suzuki, K., Sato, R., *et al.* (2007). Sterol regulatory element-binding protein-2- and liver X receptor-driven dual promoter regulation of hepatic ABC transporter A1 gene expression: mechanism underlying the unique response to cellular cholesterol status. J Biol Chem **282,** 21090–21099.

Twiddy, A.L., Leon, C.G., and Wasan, K.M. (2010). Cholesterol as a potential target for castration-resistant prostate cancer. Pharm Res **28,** 423–437.

Wang, J., Ban, M.R., Zou, G.Y., Cao, H., Lin, T., Kennedy, B.A., *et al.* (2008a) Polygenic determinants of severe hypertriglyceridemia. Hum Mol Genet **17,** 2894–2899.

Wang, X., Collins, H.L., Ranalletta, M., Fuki, I.V., Billheimer, J.T., Rothblat, G.H., *et al.* (2007). Macrophage ABCA1 and ABCG1, but not SR-BI, promote macrophage reverse cholesterol transport *in vivo*. J Clin Invest **117,** 2216–2224.

Wang, X., and Rader, D.J. (2007). Molecular regulation of macrophage reverse cholesterol transport. Curr Opin Cardiol **22,** 368–372.

Wang, Y., Rogers, P.M., Su, C., Varga, G., Stayrook, K.R., and Burris, T.P. (2008b) Regulation of cholesterologenesis by the oxysterol receptor, LXRalpha. J Biol Chem. **283,** 26332–26339.

Weiss, J.S., Kruth, H.S., Kuivaniemi, H., Tromp, G., White, P.S., Winters, R.S., *et al.* (2007). Mutations in the UBIAD1 gene on chromosome short arm 1, region 36, cause Schnyder crystalline corneal dystrophy. Invest Ophthalmol Vis Sci **48,** 5007–5012.

Zhou, C., King, N., Chen, K.Y., and Breslow, J.L. (2009). Activation of PXR induces hypercholesterolemia in wild-type and accelerates atherosclerosis in apoE deficient mice. J Lipid Res **50,** 2004–2013.

Zhou, X., Yin, Z., Guo, X., Hajjar, D.P., and Han, J. (2010). Inhibition of ERK1/2 and activation of liver X receptor synergistically induce macrophage ABCA1 expression and cholesterol efflux. J Biol Chem **285,** 6316–6326.

Zhuang, L., Kim, J., Adam, R.M., Solomon, K.R., and Freeman, M.R. (2005). Cholesterol targeting alters lipid raft composition and cell survival in prostate cancer cells and xenografts. J Clin Invest **115,** 959–968.

Address correspondence to:
William J. Fredericks, Ph.D.
Division of Urology
Department of Surgery
University of Pennsylvania
VAMC Philadelphia
University and Woodland Ave., Room A418
Philadelphia, PA 19104

E-mail: william.fredericks@uphs.upenn.edu

Received for publication May 3, 2011; received in revised form May 31, 2011; accepted June 1, 2011.